Published in "Physical Review Letters 104: 255302, 2010"
which should be cited to refer to this work.

Ramsey Interference in One-Dimensional Systems: The Full Distribution Function of Fringe Contrast as a Probe of Many-Body Dynamics

Takuya Kitagawa,[1] Susanne Pielawa,[1] Adilet Imambekov,[2] Jörg Schmiedmayer,[3] Vladimir Gritsev,[4] and Eugene Demler[1]

[1]*Physics Department, Harvard University, Cambridge, Massachusetts 02138, USA*
[2]*Department of Physics and Astronomy, Rice University, Houston, Texas 77005, USA*
[3]*Atominstitut, TU-Wien, Stadionallee 2, 1020 Vienna, Austria*
[4]*Physics Department, University of Fribourg, Chemin du Musee 3, 1700 Fribourg, Switzerland*

We theoretically analyze Ramsey interference experiments in one-dimensional quasicondensates and obtain explicit expressions for the time evolution of full distribution functions of fringe contrast. We show that distribution functions contain unique signatures of the many-body mechanism of decoherence. We argue that Ramsey interference experiments provide a powerful tool for analyzing strongly correlated nature of 1D interacting systems.

PACS numbers: 67.85.−d, 03.75.Dg

Introduction.—Recent progress in the field of ultracold atoms not only expanded our understanding of equilibrium properties of interacting 1D Bose gases [1,2] but also posed new theoretical challenges by studying far-from-equilbrium dynamics of such systems. Recent experiments addressed such questions as thermalization and integrability [3], decoherence after the splitting of two condensates [4] and spin dynamics of two-component Bose mixtures [5]. Motivation for such experiments comes not only from the basic interests in many-body dynamics [6] but also from possible applications of ultracold atoms such as quantum information processing [7] and interferometric sensing [8]. In this paper, we theoretically analyze the decoherence dynamics of Ramsey interference fringes in one-dimensional quasicondensates. Such systems have been considered for possible applications in atomic clocks and quantum-enhanced metrology [9,10]. Here we show that a Ramsey interferometer is also a powerful tool for studying many-body dynamics of low dimensional quantum systems. We find that decoherence of Ramsey fringes is strongly affected by the multimode character of one-dimensional systems. Moreover we will demonstrate that the time evolution of the full distribution function of fringe contrast provides unique signatures of this many-body decoherence mechanism [11]. The idea of using noise and distribution functions to characterize equilibrium many-body states of ultracold atoms has been discussed in several theoretical papers [12] and applied in experiments [1,13]. This Letter constitutes the first proposal to study nonequilibrium dynamics of ultracold atoms with quantum noise.

The role of interactions in Ramsey interferometers with BEC was first addressed in the pioneering paper of Kitagawa and Ueda [10]. They used the single mode approximation to predict the interaction-induced decoherence of Ramsey fringes along with the appearance of spin-squeezed states. Their work stimulated ideas for quantum-enhanced metrology that take advantage of spin-squeezed states formed in interacting BECs [9,14]. For the analysis of one-dimensional quasicondensates, however, the single mode approximation cannot be applied because these systems do not have macroscopic occupations of a single state, even at zero temperature. The non mean-field character of the multimode spin dynamics in 1D quasicondensates was first reported in experiments by Widera *et al.* [5]. However, this work did not provide a definitive demonstration of the many-body origin of Ramsey fringe decay. In the following, we argue that unambiguous signatures of the multimode decoherence are found in the full distribution function of the Ramsey fringe amplitudes. Such distribution functions should be accessible in experiments with 1D quasicondensates realized on atom chips [15], because such systems do not average over multiple tubes and thus allow the measurements of shot-to-shot fluctuations [1].

Now we describe the Ramsey sequence considered in this Letter. Here we identify two hyperfine states as spin-up and spin-down states. The Ramsey sequence is carried out as follows: (i) all spins of the atoms are prepared in the spin up state; (ii) a $\pi/2$ pulse is applied to rotate each spin into the x direction; (iii) spins freely evolve (precess) for time t; (iv) another $\pi/2$ pulse is applied to map the transverse spin component to the z direction, which is then measured. Measurements yield a net spin $\vec{S}_l$ for a segment of length l and we assume that l is smaller than the system size but large enough to contain a large number of particles $N_l \gg 1$. In such a case, the simultaneous measurements of S_l^x and S_l^y are possible, because even though operators S_l^x and S_l^y generally do not commute, the noncommutativity gives only corrections of the order of $1/\sqrt{N_l}$ relative to the average values [16]. Commutativity of S_l^x and S_l^y implies, in particular, that we can define the joint distribution function $P_l^{x,y}$ for the two transverse spin components S_l^x and S_l^y. In experiments, measurements of $P_l^{x,y}$ are possible by mapping the spin orientations in x-y plane to z direction by $\pi/2$ pulse, followed by the local measurements of S_z [17]. S_l^x and S_l^y as well as the magnitude of spin

$S_l^\perp = \sqrt{(S_l^x)^2 + (S_l^y)^2}$ can be found by taking the integration over l. The analytic solution for the time evolution of $P_l^{x,y}$ constitutes the main result of this Letter. In addition, we assume that l is larger than the spin healing length ξ_s, so we can use Tomonaga-Luttinger liquid approach to describe the collective spin dynamics (see also below). For simplicity we work in the rotating frame of the Larmor precession, and consider the spins before the last $\pi/2$ pulse. Then the amplitude of Ramsey fringes, as it is conventionally defined, corresponds to S_l^x.

Our main results are summarized in Fig. 1 and can be understood from the following physical arguments. Strong fluctuations present in 1D systems forbid the existence of the long range coherence [18], and spatial fluctuations coming from different wavelengths strongly affect the dynamics in one dimension. Among those, fluctuations with wavelengths longer than the integration length l rotate $\vec{S}_l$ as a whole. So they decrease S_l^x but not the magnitude of the spin $S_l^\perp = \sqrt{(S_l^x)^2 + (S_l^y)^2}$. Fluctuations with wavelengths shorter than l decrease both S_l^x and $S_l^\perp$ simultaneously. Figures 1(a) and 1(b) show the situation where fluctuations with wavelength larger than l dominate the dynamics. In (a), we see that the magnitude of the spin $S_l^\perp$ decays only slightly from the initial state but the direction of the spin is randomized during the time evolution. Note that in this case the distribution function of S_l^x has a very peculiar shape with two peaks at large positive and negative values. We call this regime, "spin diffusion" regime. Figures 1(c) and 1(d) show the situation where fluctuations with wavelengths shorter than l dominate. In this case $S_l^\perp$ and S_l^x decay in the same time scale. We call this regime, "spin decay" regime. Below we argue that the crucial parameter of the system is a dimensionless ratio proportional to the length of the integration region $l_0 = \frac{\pi^2 l}{4K_s\xi_s}$. When $l_0 \leq 1$ the system is in the spin diffusion regime and the other limit $l_0 \gg 1$ is the spin decay regime.

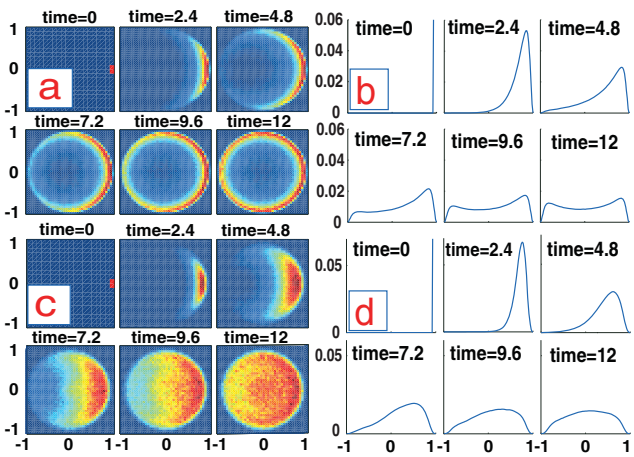

FIG. 1 (color). (a),(c) Evolution of joint FDF $P_l^{x,y}$ with short integration length $l/\xi_s = 10$ [top, (a)] and long integration length $l/\xi_s = 30$ [bottom, (c)]. (b),(d) Corresponding FDF for spin x, P_l^x with short integration length $l/\xi_s = 10$ [top, (b)] and long integration length $l/\xi_s = 10$ [bottom, (d)]. Here $L/\xi_s = 200$, $K_s = 20$. Time is measured in units of ξ_s/c_s.

Model.—Following the first $\pi/2$ pulse we have a two-component Bose mixture with equal densities of both species. Tomonaga-Luttinger liquid (TLL) approach, which we use in this paper, focuses on the linearly dispersing modes in the low energy part of the spectrum. For simplicity, we consider the case when the interaction strength among particles with spin up is the same as that among particles with spin down. This condition can be reached for the hyperfine states $|F = 1, m_F = -1\rangle$ and $|F = 2, m_F = +1\rangle$ of ^{87}Rb that are commonly used in experiments [1,5]. When this is the case, the charge and spin parts of the Tomonaga-Luttinger Hamiltonian decouple and the spin part of the Hamiltonian is given by [18]

$$H_s = \frac{c_s}{2}\int_{-L/2}^{L/2} dr\left[\frac{K_s}{\pi}(\nabla\phi_s(r))^2 + \frac{\pi}{K_s}n_s^2(r)\right]. \quad (1)$$

Here L is the total system size, $n_s(r)$ describes the local spin imbalance (i.e., z component of the spin) $n_s = \psi_\alpha^\dagger(\frac{1}{2}\sigma_{\alpha\beta}^z)\psi_\beta$ where $\psi_\alpha^\dagger$ is the creation operator of a particle with spin α and σ^a is a component of Pauli matrix. $\phi_s(r,t)$ describes the direction of the transverse spin component $\rho e^{i\phi_s} = \psi_\alpha^\dagger(\frac{1}{2}\sigma_{\alpha\beta}^+)\psi_\beta$ with ρ being the average density for each species and $\sigma^+ = \sigma^x + i\sigma^y$. Variables n_s and ϕ_s obey canonical commutation relations $[n_s(r), \phi_s(r')] = -i\delta(r - r')$. K_s is spin Luttinger parameter representing interaction strength [5], and c_s is spin-wave velocity. In the weak interaction limit, these parameters are related to physical parameters as $c_s = \sqrt{g_s\rho/m}$, $\xi_s = \frac{\pi c_s}{g_s\rho}$ and $K_s = \xi_s\rho/2$, where m is the mass of the particle and $g_s = \frac{4\pi^2\hbar^2}{m}\frac{a_{\uparrow\uparrow}+a_{\downarrow\downarrow}-2a_{\uparrow\downarrow}}{2}$ is the interaction strength in spin channel where $a_{\alpha,\beta}$ refers to s-wave scattering length between hyperfine spin α and β. In this Letter, we focus on the regime $g_s > 0$ when the system is miscible. Our approach can be extended to $g_s < 0$ but will be limited to times before z magnetization per atom becomes of the order of 1. Harmonic Hamiltonian (1) can be diagonalized by going to momentum space, and it takes the form

$$H_s = \sum_{k\neq 0} c_s|k|b_{s,k}^\dagger b_{s,k} + \frac{c_s\pi}{2K_s}n_{s,0}^2. \quad (2)$$

The first and second term of (2) correspond to $k \neq 0$ and $k = 0$ part of the Hamiltonian, respectively, and $n_{s,k}$ represents the Fourier transform of $n_s(r)$. This Hamiltonian has a momentum cutoff set by the inverse of the spin healing length ξ_s^{-1}. The operators $b_{s,k}^\dagger$ create spin excitations with momentum k, and these spin excitations are the main focus of our study.

Transverse part of the spin operator $\vec{S}_l$ is given by

$$S_l^x = \int_{-l/2}^{l/2} dr\rho\cos(\phi_s(r)), \quad S_l^y = \int_{-l/2}^{l/2} dr\rho\sin(\phi_s(r)). \quad (3)$$

When describing spin dynamics, one typically considers the time evolution of expectation values $\langle S_l^a(t)\rangle$. However important information is also contained in the shot-to-shot fluctuations of $S_l^a(t)$. Such quantum noise is captured by the full distribution functions (FDF) of spin operators, $P_l^a(\alpha, t)$ [11]. In particular, high moments of $S_l^a(t)$ can be obtained from these FDFs $P_l^a(\alpha, t)$. Physically, $P_l^a(\alpha, t)d\alpha$ is the probability that a single measurement of the spin operator S_l^a at time t gives a value between α and $\alpha + d\alpha$. In experiments, $P_l^a(\alpha, t)$ can be obtained by making histograms of the measurement results of $S_l^a(t)$.

To describe the time evolution of spin operators (3), we need to characterize the initial state of the system after the first $\pi/2$ rotation [19]. Classically one expects the initial state to be the eigenstate of $\phi_s(r)$ with eigenvalue zero for all r. However, such a state is unphysical in quantum mechanics since it leads to infinite uncertainty of the conjugate variable $n_s(r)$, and thus, to infinite energy. It is more sensible to consider an initial state that has a small uncertainty in ϕ_s at the expense of enhanced fluctuations in n_s, which is a squeezed state in the ϕ_s, n_s variables [5,21]. We observe that the spin of each individual atom is independently rotated by the first $\pi/2$ pulse into the x direction, so the initial state satisfies $\langle S^z(r)S^z(r')\rangle = \frac{\rho}{2}\,\delta(r - r')$. Thus we find a Gaussian state for the spin operator S^z in momentum space

$$|\psi_0\rangle = \frac{1}{\mathcal{N}} \exp\Big(\sum_{k\neq 0} W_k b_{s,k}^\dagger b_{s,-k}^\dagger\Big)|0\rangle|\psi_{s,k=0}\rangle, \qquad (4)$$

where $2W_k = (1 - \alpha_k)/(1 + \alpha_k)$, $\alpha_k = |k|K_s/\pi\rho$ and $\mathcal{N}$ is the overall normalization of the state. For the uniform part of the spin operator we also have a squeezed state $\langle n_{s,0}|\psi_{s,k=0}\rangle = \exp(-1/(2\rho)n_{s,0}^2)$. We note that model (1) has a short distance cutoff, so the δ function in $\langle S^z(r)S^z(r')\rangle$ should be understood as rounded off on the scale of ξ_s, which is implicit in the momentum cutoff in Eq. (4).

The time evolution of the state (4) leads to $W_k \to W_k e^{2ic_s|k|t}$. From the resulting expression for the state at time t, one can readily calculate the decay of Ramsey fringes given by $\langle S_l^x(t)\rangle$, which is independent of integration length l (See also [5,21]). To calculate the time evolution of FDF, we define instantaneous annihilation operators $\gamma_{ks}(t)$ such that applying $\gamma_{ks}(t)$ on the state $\exp(W_k e^{2ic_s|k|t} b_{s,k}^\dagger b_{s,-k}^\dagger)|0\rangle$ gives zero. Using operators $\gamma_{ks}(t)$, one can apply the approach described in Refs. [1,11] for calculating distribution functions of equilibrium systems. After direct calculation we find [20]

$$P_l^{x,y}(\alpha, t) = \prod_k \int_{-\infty}^{\infty} e^{-\lambda_{rsk}^2/2} d\lambda_{rsk} \int_{-\pi}^{\pi} d\lambda_{\theta sk} \times \delta\Big(\alpha - \rho \int_{-l/2}^{l/2} dr e^{i\chi(r,t,\{\lambda_{jsk}\})}\Big), \qquad (5)$$

$$\chi(r, t, \{\lambda_{jsk}\}) = \sum_k \lambda_{rsk}\sqrt{\frac{\langle|\phi_{s,k}(t)|^2\rangle}{L}}\sin(kr + \lambda_{\theta sk}),$$

$$\langle|\phi_{s,k\neq 0}|^2\rangle = \Big(\frac{\pi\rho}{|k|K_s}\Big)^2 \frac{\sin^2(c_s|k|t)}{2\rho} + \frac{\cos^2(c_s|k|t)}{2\rho},$$
$$\langle|\phi_{s,k=0}|^2\rangle = \frac{1}{2\rho} + \Big(\frac{c_s\pi t}{K_s}\Big)^2 \frac{\rho}{2}, \qquad (6)$$

where the real and imaginary part of α corresponds to x and y component of $\vec{S}_l$, respectively. Equation (5) and (6) allow a simple physical interpretation. Function $\chi(r, t, \{\lambda\})$ defines the local direction of transverse magnetization, which results from the summation over spin-wave like modes $\sin(kr + \lambda_{\theta sk})$. Amplitudes of individual modes are given by the time dependent expectation values $\langle|\phi_{s,k}(t)|^2\rangle$ and by the set of random variables λ_{rsk} drawn from a Gaussian ensemble. Equation (5) and (6) reflect the key feature of dynamics of the quadratic Luttinger model (1): an initial Gaussian state for $\phi_{s,k}$ remains Gaussian at all times.

Time evolution of $\langle|\phi_{s,k}(t)|^2\rangle$ following the first $\pi/2$ rotation can be understood as the free dynamics of a harmonic oscillator. From the conjugate nature of $\phi_{s,k}$ and $n_{s,k}$, we find $\langle|\phi_{s,k}(0)|^2\rangle = \frac{1}{4}\frac{1}{\langle|n_{s,k}(0)|^2\rangle} = \frac{1}{2\rho}$ at $t = 0$. Subsequently $\langle|\phi_{s,k}(t)|^2\rangle$ oscillates between the minimal value in the initial state and some maximum value $\langle|\phi_{s,k}|^2\rangle_{\max}$ at the frequency of a harmonic oscillator $c_s|k|$. $\langle|\phi_{s,k}|^2\rangle_{\max}$ can be estimated from energy conservation. Since the initial state was squeezed with respect to ϕ_{sk}, most of the energy of the mode is stored in the interaction term $|n_{s,k}|^2$. Therefore the total energy of the harmonic oscillator for momentum k can be approximated by $\frac{\pi c_s\rho}{K_s}$, which in turn gives $\langle|\phi_{s,k}|^2\rangle_{\max} \sim \frac{2\pi^2\rho}{K_s^2k^2} = \frac{1}{2\rho}(\frac{\pi\rho}{|k|K_s})^2$. These considerations lead to the dynamics of phase fluctuation amplitude of the form in (6). We note that the spin fluctuations are dominated by small momentums since the maximum fluctuation amplitude is suppressed as $1/k^2$ for large momentum. This justifies our analysis based on the Tomonaga-Luttinger theory.

Results of numerical plots based on Eq. (5) and (6) are shown in Fig. 1. In Fig. 2(a) we also present the distribution function $P_l^\perp$ of the magnitude square of the integrated spin $(S_l^\perp)^2$, which clearly demonstrates the difference between the "spin diffusion" and spin decay regimes. The character of these distribution functions can be understood from the following arguments. We first discuss the "spin diffusion" regime, where the characteristic wavelength of spin fluctuations is longer than the integration length l [Figs. 1(a) and 1(b)]. In this regime, all spins within l essentially point in the same direction and $S_l^\perp$ remains large even after a long time evolution. Thus we find a peak at $(S_l^\perp)^2 \approx 1$ in the distribution function $P_l^\perp$ (red line). In the other regime of spin decay [Figs. 1(c) and 1(d)], the typical length scale of spin fluctuations is shorter than the integration length l.

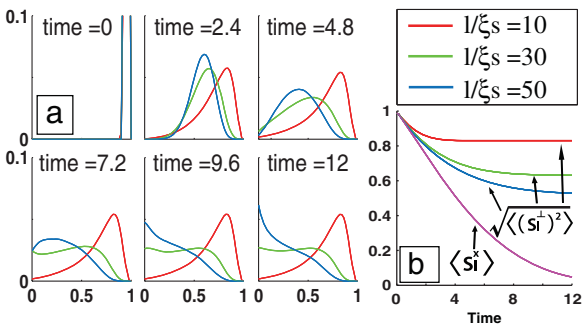

FIG. 2 (color). (a) Time evolution of the distribution $P_l^\perp$ for the magnitude of spin $(S_l^\perp)^2$. (b) time evolution of $\langle S_l^x \rangle$ and $\sqrt{\langle (S_l^\perp)^2 \rangle}$ with various integration length $l/\xi_s = 10, 30, 50$. Here we set $K_s = 20$, $L/\xi_s = 200$.

In this case, integration of spins over l is akin to taking a random walk in 2D plane and accordingly, the distribution for $(S_l^\perp)^2$ approaches exponential form with a peak at $(S_l^\perp)^2 = 0$ in $P_l^\perp$ (blue line). In the intermediate regime, we observe two peak structure for $P_l^\perp$, where the distribution exhibits both characteristic peaks (green line). We can understand the condition that separates these spin decay and spin diffusion type dynamics in the following way. Deviation of spin angles at $r = l$ relative to $r = 0$ can be estimated from $\Delta\chi \approx \frac{1}{\sqrt{L}} \sum_k \lambda_{rsk} \sqrt{\langle |\phi_{s,k}|^2 \rangle_{\max}} \sin(kl)$. A typical magnitude of $\Delta\chi$ is given by $\langle (\Delta\chi)^2 \rangle$ where the average is taken over fluctuations of λ_{rsk}. The factor $\sin(kl)$ in $\Delta\chi$ effectively limits momentum integration range to $k > 2\pi/l$, so $\langle (\Delta\chi)^2 \rangle \approx \frac{\pi^2 l}{2K_s \xi_s}$. When $\langle (\Delta\chi)^2 \rangle^{1/2}$ is smaller than 2π the system is in the spin diffusion regime. When $\langle (\Delta\chi)^2 \rangle^{1/2}$ becomes of the order of 2π and larger, the system enters the spin decay regime. The crossover takes place around $\frac{\pi^2 l}{4K_s \xi_s} \sim 1$.

In the spin diffusion regime, the dynamics of $S_l^\perp$ and S_l^x display different time scales as can be seen in Fig. 2(b). In order to understand this separation of time scale, we note that the magnitude of the integrated spin $S_l^\perp$ is only affected by fluctuations with short wavelengths, $\lambda < l$, for which dynamics takes place at short time scale. Hence $\langle S_l^\perp \rangle$ decays until the time $t_\perp \approx 2\pi l/c_s$ [see Eq. (6)] and then it reaches a saturated value. On the other hand, S_l^x is affected by excitations of all wavelengths, so $\langle S_l^x \rangle$ decays until it reaches 0. These behaviors are shown in Fig. 2(b), where we compared the decay of $\langle S_l^\perp \rangle$ for various segment length l and $\langle S_l^x \rangle$. Nontrivial time evolution of the distribution functions P_l^x, $P_l^{x,y}$ and especially the striking contrast of the spin diffusion and spin decay regimes should provide unique signatures of the non-mean-field character and multimode dynamics of 1D systems.

Summary.—We provided a theoretical analysis of Ramsey interference experiments with 1D quasicondensates, and showed that the time evolution of the full distribution function contains unique signatures of the many-body dynamics in one dimension.

This work was supported by NSF grant DMR-0705472, Harvard MIT CUA, DARPA OLE program, AFOSR MURI, and Swiss NSF.

[1] S. Hofferberth *et al.*, Nature Phys. **4**, 489 (2008).
[2] B. Paredes *et al.*, Nature (London) **429**, 277 (2004); T. Kinoshita, T. Wenger, and D. S. Weiss, Science **305**, 1125 (2004); A. H. van Amerongen *et al.*, Phys. Rev. Lett. **100**, 090402 (2008).
[3] T. Kinoshita, T. Wegner, and D. Weiss, Nature (London) **440**, 900 (2006).
[4] S. Hofferberth *et al.*, Nature (London) **449**, 324 (2007).
[5] A. Widera *et al.*, Phys. Rev. Lett. **100**, 140401 (2008).
[6] I. Shvarchuck *et al.*, Phys. Rev. Lett. **89**, 270404 (2002); P. Calabrese and J. S. Caux, Phys. Rev. Lett. **98**, 150403 (2007); M. A. Cazalilla, Phys. Rev. Lett. **97**, 156403 (2006); M. Rigol, V. Dunjko, and M. Olshanii, Nature (London) **452**, 854 (2008); E. Altman *et al.*, Phys. Rev. Lett. **95**, 020402 (2005); A. Polkovnikov and V. Gritsev, Nature Phys. **4**, 477 (2008); U. Schollwock, Rev. Mod. Phys. **77**, 259 (2005).
[7] T. Calarco *et al.*, Phys. Rev. A **61**, 022304 (2000).
[8] A. D. Cronin, J. Schmiedmayer, and D. E. Pritchard Rev. Mod. Phys. **81**, 1051 (2009).
[9] A. S. Sorensen and K. Molmer, Phys. Rev. Lett. **83**, 2274 (1999); A. Sorensen *et al.*, Nature (London) **409**, 63 (2001).
[10] M. Kitagawa and M. Ueda, Phys. Rev. A **47**, 5138 (1993).
[11] A. Polkovnikov, E. Altman, and E. Demler, Proc. Natl. Acad. Sci. U.S.A. **103**, 6125 (2006); A. Imambekov, V. Gritsev, and E. Demler, Phys. Rev. A **77**, 063606 (2008); V. Gritsev *et al.*, Nature Phys. **2**, 705 (2006).
[12] E. Altman, E. Demler, and M. D. Lukin, Phys. Rev. A **70**, 013603 (2004); K. Eckert *et al.*, Nature Phys. **4**, 50 (2008); A. Lamacraft, Phys. Rev. A **76**, 011603(R) (2007).
[13] Z. Hadzibabic *et al.*, Nature (London) **441**, 1118 (2006).
[14] A. M. Rey *et al.*, Phys. Rev. A **77**, 052305 (2008).
[15] R. Folman *et al.*, Phys. Rev. Lett. **84**, 4749 (2000); R. Folman *et al.*, Adv. At. Mol. Phys. **48**, 263 (2002); J. Fortagh and C. Zimmermann, Rev. Mod. Phys. **79**, 235 (2007).
[16] A. Polkovnikov, Europhys. Lett. **78**, 10 006 (2007).
[17] G. B. Jo *et al.*, Science **325**, 1521 (2009).
[18] T. Giamarchi, *Quantum Physics in One Dimension* (Oxford University Press, Oxford, United Kingdom, 2004).
[19] Corrections due to small difference in the s-wave scattering lengths among spin ups and downs introduce temperature dependence, but they do not lead to qualitative changes of distribution functions [20].
[20] T. Kitagawa *et al.* (to be published).
[21] R. Bistritzer and E. Altman, Proc. Natl. Acad. Sci. U.S.A. **104**, 9955 (2007); A. A. Burkov, M. D. Lukin, and E. Demler, Phys. Rev. Lett. **98**, 200404 (2007); I. E. Mazets and J. Schmiedmayer, Eur. Phys. J. B (2009).